Colloid Polym Sci 275:274–283 (1997)
© Steinkopff Verlag 1997

ORIGINAL CONTRIBUTION

R.H. Ottewill
A.B. Schofield
J.A. Waters
N.St.J. Williams

Preparation of core-shell polymer colloid particles by encapsulation

Received: 12 September 1996
Accepted: 18 September 1996

Prof. Dr. R.H. Ottewill (✉)
A.B. Schofield · J.A. Waters
School of Chemistry
University of Bristol
Bristol BS8 1TS, United Kingdom

N.St.J. Williams
ICI Paints
Wexham Road
Slough, Berkshire SL2 5DS
United Kingdom

Abstract By means of heterocoagulation anionic poly-[styrene] particles were coated with smaller electrosterically stabilised cationic particles of poly-[butyl methacrylate]. On heating the heterocoagulated units 45 °C above the glass transition temperature of poly-[butyl methacrylate], as predicted theoretically, the latter polymer spread over the surface of the poly-[styrene] particle to give a composite particle with a core-shell structure. It was found that the extent of packing of the small particles on the larger core particle was a critical feature of the coating process.

Key words Heterocoagulation – polymer colloids – poly-[styrene] – poly-[butylmethacrylate] – encapsulation – core-shell particles

Introduction

The use of amidine initiators in polymerisation reactions has been known since 1952 [1] and a synthesis of these initiators was published in 1963 [2]. Emulsion polymerisation using them was described in 1966 [3]. In the 1970's the preparation of monodisperse cationic polystyrene, PS, latices by an emulsifier-free route was published [4–6]. These latices were used for the study of heterocoagulation and scanning electron microscopy was used to show [7] that 2 μm anionic polystyrene latex particles could be coated with 0.5 μm cationic particles to form a close-packed layer on the surface of the larger particle. The kinetic aspects of the heterocoagulation process were also examined [8, 9]. Recently, the possibility of using heterocoagulation for the purpose of forming composite particles has been initiated by several groups of authors [10–16] since it offers the possibility of better control for certain types of composite particle morphology, e.g., core-shell. Whereas, with preparations using both mixed monomers and sequential polymerisation the outcome from emulsion and dispersion polymerisation has not always been predictable [17–31].

Moreover, recently a number of publications have appeared suggesting theories, based on the surface energies of the polymers, which indicate possible methods of producing particles with well-defined morphology either by engulfment or by encapsulation [10, 11, 16, 32–37]. These models suggest that for core-shell morphology heterocoagulation could be used to coat one particle, usually the larger with a high glass-transition temperature, T_g, with smaller particles of another polymer having a low T_g. On the basis of the theories provided the surface energies are correctly chosen, then on heating the system above the T_g of the smaller particles these should spread over the larger to form a continuous shell. The overall procedure is illustrated schematically in Fig. 1.

In the present work the core particle used was composed of PS with a negatively charged surface. The second latex, the coating latex, contained small cationic particles of poly(butyl methacrylate), PBMA. These particles, which

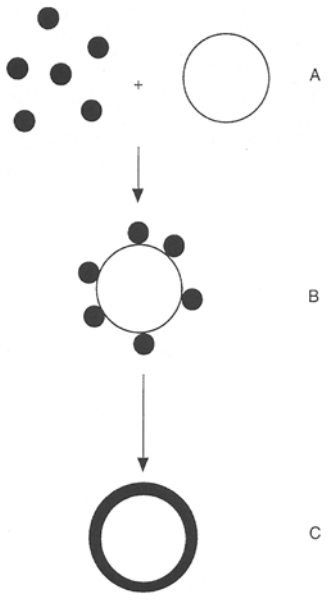

Fig. 1 Schematic flow chart for the process of forming composite core-shell polymer colloid particles by encapsulation

also had a steric layer of nonionic polymer grafted onto the surface, were heterocoagulated onto the polystyrene particles. The nonionic polymer continued to act as a stabiliser for the resulting cluster. The latter was then heated approximately 45 °C above the glass transition temperature, T_g, of PBMA. At this stage the PBMA spread over the surface of the core PS particles; colloid stability and freeze-thaw experiments indicated that the nonionic polymer migrated to the shell surface and continued to act as a steric stabilising layer.

Theory

Some theoretical concepts

From the basic mechanism depicted in Fig. 1 some consideration can be made of the interfacial energy and packing requirements needed to obtain effective encapsulation.

Interfacial energy conditions

For simplicity, as shown in Fig. 2, only two particles will be considered in the analysis, a small encapsulating particle, E, of radius R_E, with an interfacial tension against water, γ_{EW}, and a larger core particle of radius R_C, with an interfacial tension, γ_{CW}. Following encapsulation as shown in Fig. 2 a particle of radius, R_T, is obtained with an interfacial energy between the core and the encapsulating shell of γ_{CE}; the interfacial energy of the outer shell against water is assumed to remain as γ_{EW}.

From the work described in previous papers [10–12] the encapsulated composite particles would be expected to have a lower total interfacial energy than the two separate particles if,

$$\frac{\gamma_{CW} - \gamma_{CE}}{\gamma_{EW}} > \frac{1 - \phi_E^{2/3}}{\phi_C^{2/3}} \tag{1}$$

where ϕ_E and ϕ_C are fractional volumes defined by,

$$\phi_C = V_C/V_T \quad \text{and} \quad \phi_E = V_E/V_T$$

with

$$\phi_C + \phi_E = 1$$

where V_E and V_C are respectively the volumes of the encapsulating particle and the core particle and V_T is the volume of the final composite particle.

It has also been suggested that only partial spreading of polymer (E) on the surface of particle (C) would be obtained [16, 36, 37] if

$$-1 < \frac{\gamma_{CW} - \gamma_{CE}}{\gamma_{EW}} < 1 \, . \tag{2}$$

Alternatively the left-handside of expression (1) can be written in terms of the contact angle (θ), namely

$$\frac{\gamma_{CW} - \gamma_{CE}}{\gamma_{EW}} = \cos\theta$$

i.e., in terms of Young's equation.

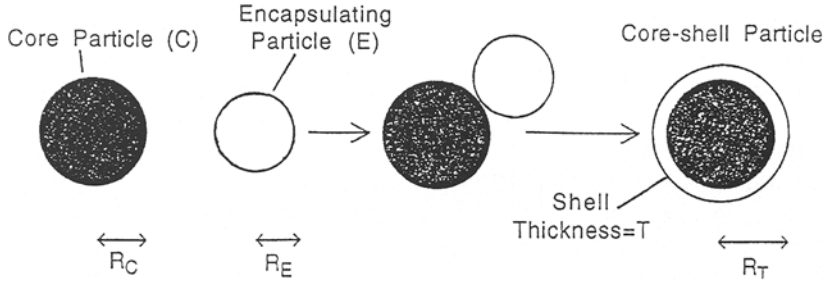

Fig. 2 Schematic illustration showing the heterocoagulation of a core particle of radius, R_c, with an encapsulating particle of radius, R_E, followed by spreading to form an encapsulated unit of radius R_T

© Steinkopff Verlag 1997

Thus when $\cos\theta = 1$, complete spreading should be achieved and when the left-handside of the expression (1) has a value less than 1, the spreading is likely to be incomplete (i.e., $\theta > 0$).

Also, with an encapsulating particle much smaller than the core particle ($\phi_E \ll \phi_C$)

$$\frac{1-\phi_E^{2/3}}{\phi_C^{2/3}} \rightarrow 1 .$$

These considerations indicate that to promote spreading of the polymer particle on the surface of the larger particle, it will be preferable to arrange conditions such that the interfacial energy expression $(\gamma_{CW} - \gamma_{CE})/\gamma_{EW}$ has a value which either approaches or exceeds 1.

The value of the interfacial energy expression increases with:

i) increasing γ_{CW}, that is with a decrease in the surface energy, γ_C, of the core particle;
ii) decreasing γ_{CE}, which occurs if the surface energy of the encapsulating particle becomes similar to that of the core particle;
iii) decreasing γ_{EW}, that is with an increase in the surface energy of the encapsulating particle.

Choice of number of encapsulating particles

In the previous section the consideration of interfacial energy conditions was based upon heterocoagulation of one E particle with the core particle. When the core particles are larger than the encapsulating particles, then in order to obtain a continuous shell it is necessary to pack a number of particles on the surface of each core particle as illustrated in Fig. 1. Consequently the optimum number of particles on the surface for optimum shell formation on the core particle also needs to be considered.

Control of shell thickness

One approach is to consider the thickness of the polymer shell, T, after encapsulation has occurred, which is given by,

$$T = R_T - R_C$$

so that the volume of material in the shell is given by,

$$4\pi(R_T^3 - R_C^3)/3 .$$

In order to achieve this result the number of encapsulating particles required, N_i, is given by

$$R_T^3 = N_i R_E^3 + R_C^3$$

and by conservation of volume then,

$$R_T = (N_i R_E^3 + R_C^3)^{1/3}$$

and by conservation of mass,

$$R_T = \left(\frac{\rho_E N_i R_E^3 + \rho_C R_C^3}{\rho_T}\right)^{1/3} .$$

Close packing on the surface

On the basis of hexagonal close-packing of the E particles on the surface and for simplicity assuming that the surface is planar, i.e., assuming that the core radius is much larger than that of the encapsulating particle, we obtain,

$$N_{sat} = \frac{2\pi}{\sqrt{3}}\left|1 + \frac{R_C}{R_E}\right|^2$$

where N_{sat} is the number of particles required to form a close-packed particulate monolayer [38].

Consideration of the stabilising layer

In the present work the E particles were both electrostatically and sterically stabilised. It was anticipated that after encapsulation the hydrophilic polymer used as the steric stabiliser would take up a position on the outside of the shell so as to be in contact with the water. It is also assumed that this polymer would want to take up the same arrangement on the core-shell particle as it had on the original encapsulating particles. This situation is possible when the surface area of the composite particle is equal to the combined surface areas of the encapsulating particles that formed it. The number concentration at which this occurs is defined as N^* i.e., such that,

$$N^* R_E^2 = R_T^2$$

also

$$R_T^3 = (N^*) R_E^3 + R_C^3$$

and

$$N^*[\sqrt{N^*} - 1] = \left|\frac{R_C}{R_E}\right|^3 \qquad (3)$$

and hence values for N^* can be found for given values of (R_C/R_E).

Number ratios of the two particle types, can be calculated from,

$$\frac{N_E}{N_C} = \frac{W_E P_E \rho_C R_C^3}{W_C P_C \rho_E R_E^3}$$

where W_E and W_C are respectively the weight of dispersions with particle weight fraction P_E and P_C with particles of density ρ_E and ρ_C.

Experimental

Materials

All water used in latex preparation and experiments was distilled before use. The styrene monomer was BDH material. Butyl methacrylate was obtained from the Aldrich Chemical Company. Both monomers were purified by distillation at 50 °C to 60 °C in an atmosphere of nitrogen at reduced pressure and kept in a refrigerator prior to use.

Ammonium persulphate, which was BDH Analar grade material was recrystallised before use. The cationic initiator 2,2′-azobis-(2-amidinopropane) dihydrochloride (ABA.2HCl) was supplied by the Wako Chemical Company under the trade name V50. Sodium chloride was a BDH Analar grade material.

The polymeric stabiliser methoxy polyethyleneglycol methacrylate 2000 (MeOPEGMA) was supplied as 60% solution in water by ICI Paints, Slough, England. Preparation of this stabiliser has been previously described [39,40].

Preparation of polystyrene latices

The PS latices were charge stabilised and prepared using an emulsifier-free method similar to that previously published [41]. The polymerisation was carried out in a five-necked, round-bottomed flask containing a glass stirrer with a PTFE paddle, a constant flow of nitrogen and a water-cooled reflux condenser. The flask was maintained at 70 °C by immersion to the neck in a thermostatted oil bath. Into this flask was placed 60 ml of styrene monomer and 540 ml of distilled water. The mixture was stirred at 350 rpm and a constant flow of nitrogen was passed through it. Then 0.48 g of $(NH_4)_2S_2O_8$ initiator, dissolved in 20 ml of water, was added to the system. Polymerisation was allowed to proceed for 24 h. The final latex was filtered through glass wool into well-boiled Visking dialysis tubing and dialysed against distilled water to remove residual monomer, oxidation products and salts.

Preparation of poly(butyl methacrylate) latices

This preparation was carried out using a similar procedure to that used for the PS latex. Into the flask was placed 40 ml of butyl methacrylate monomer, 360 ml of water, 1.23 g of sodium chloride and 6.3 g of a 60% w/w solution of the MeOPEGMA; these reactants were allowed to thermally equilibrate at 70 °C. To this system was then added 0.32 g of the cationic initiator, ABA.2HCl, and then the reaction was left to proceed for 24 h. The resulting latex was filtered through glass wool into well-boiled Visking dialysis tubing and then dialysed against distilled water. This latex was also cleaned by centrifugation. After spinning down the particles the resultant supernatant was replaced with clean solvent. This procedure was repeated 10 times in order to remove excess stabiliser. The resulting particles were stable both to high electrolyte concentrations and to freeze-thaw conditions, both indications that the particles were sterically stabilised.

Preparation of encapsulated particles

In order to follow as closely as possible the mechanisms formulated in the theoretical section it was necessary to control the electrolyte concentration and the ratio,

$$\frac{\text{number concentration of small cationic particles}}{\text{number concentration of larger anionic particles}}.$$

For these experiments the conditions corresponding to N_{SAT} and N^* were of particular interest.

The number concentrations for each separate latex were obtained from their measured mass fractions. Mixtures of particles at the appropriate electrolyte and number concentrations (see Table 1) were prepared and then thoroughly shaken; the systems were then allowed to equilibrate for 24 h. Then, after 20 min in an ultrasonic bath to break up any flocs formed on standing, the flask containing the mixed system was placed in a thermostatted oil bath which had been preheated to 70 °C. It was maintained at this temperature for 24 h. This temperature was chosen as it was above the average T_g of PBMA namely, 21–29 °C, mean 25 °C [42, 43], but below that of PS, 106 °C [43].

Electrophoretic mobility

The electrophoretic mobilities of the particles from the separate latices and the encapsulated particles were measured as a function of pH and electrolyte concentration using a Pen Kem Inc. System 3000 electro-kinetic analyser.

Electron microscopy

Samples of the particles of PS were spotted onto nitrocellulose films supported by copper grids. In the case of

© Steinkopff Verlag 1997

Table 1 Particle encapsulation

Number ratio used in experiment	Calculated composite particle radius/nm	Measured composite radius/nm†	N
		598	O
8.4	629	661	$N^*/2$
16.8	657	667	N^*
33.5	707	678	$2N^*$
50.3	750	671	$3N^*$
67.0	789	664	$4N^*$
81.4	820	680	N_{sat}

† Particle size determined by disc photosedimentometry. Electrolyte concentration. 10^{-5} mol dm^{-3} sodium chloride.

PBMA particles, since they were unstable in the electron beam, carbon replicas of the particles were prepared for examination. Both particles and replicas were examined by transmission electron microscopy using a JEOL 100C instrument. The particle size distributions were obtained from measurements of ca 800 particles on photographic enlargements of the micrographs using a Carl Zeiss TGZ 3 particle size analyser (see Table 2). Heterocoagulated clusters were also examined as carbon replicas.

In addition the particle clusters were examined after freeze drying in the following manner. A thin mica sheet was dipped into the sample and then drained using a paper towel so as to leave a thin film of the sample, approximately 20 μm thick. The mica sheet was then placed rapidly on to a brass block which had been cooled to liquid nitrogen temperature; this froze the sample quickly. The frozen sample was transferred to a cryostat at $-60\,^{\circ}$C and pumped under vacuum for five hours to remove ice. The remaining particles were then coated with tungsten and examined by both transmission and scanning electron microscopy.

Disc centrifuge photosedimentometry

As in previous work [16] a Brookhaven spinning disc centrifuge, type DCP-1000 Particle-Sizer, was used for the determination of particle size and to obtain an estimate of the particle size distribution.

Results

Electron microscopy

Figure 3 shows transmission electron micrographs of the PS-latex and the PBMA latex used in the present work. As anticipated from previous work [44], PS has more electron contrast and therefore the PS particles appear darker than the PBMA particles. This is a very useful feature as it can be used to infer the location of the different polymers in composite particles.

Figure 4 shows a replica of a freeze-dried preparation resulting from the heterocoagulation of the cationic PBMA particles with the anionic PS particles in 10^{-5} mol dm^{-3} sodium chloride solution (Table 1). The small particles adsorb onto the larger particle to give a "raspberry-like" structure. The conditions for this experiment were such as to anticipate an N_{sat} packing on the particle surface. When the aqueous mixture was heated to 70 °C and the resulting heterocoagula, freeze-dried and examined by electron microscopy the replicas gave the type of results shown in Fig. 5. Although some flow of the PBMA particles occurred a rough uneven surface was produced and complete spreading of the PBMA did not occur; the PBMA particles essentially remained as separate units.

However, when the concentration of PBMA particles was adjusted to correspond to N^* a different situation was encountered. Spreading occurred much more readily and a smooth coating of PBMA was obtained on the PS particles. Transmission electron micrographs of the particles obtained by this procedure are shown in Fig. 6. Around the PS-core particle, which appears black on the micrograph, the more electron-transparent shell of PBMA can be clearly seen. Evidence for this core-shell structure is also supported by small angle neutron scattering experiments on this system [45].

Table 2 Characterization of latices

Latex material	Charge	Electron microscopy Diameter	Coeff. of var. on mean	Disc centrifuge Photosediment only Wt. av.	Wt./no av.	Photon correlation spectroscopy Diameter	Std. dev.	Density/ g cm^{-3}
PS	Anionic	1202 nm	5.0%	1197 nm	1.019	1139 nm	0.17	1.054
PBMA	Cationic†	334 nm	5.1%	271 nm	1.015	289 nm	0.13	1.058
Composite	Anionic†	1342 nm	5.3%	1416 nm	1.045	–	–	1.038

† Also had a steric layer of MeOPEGMA.

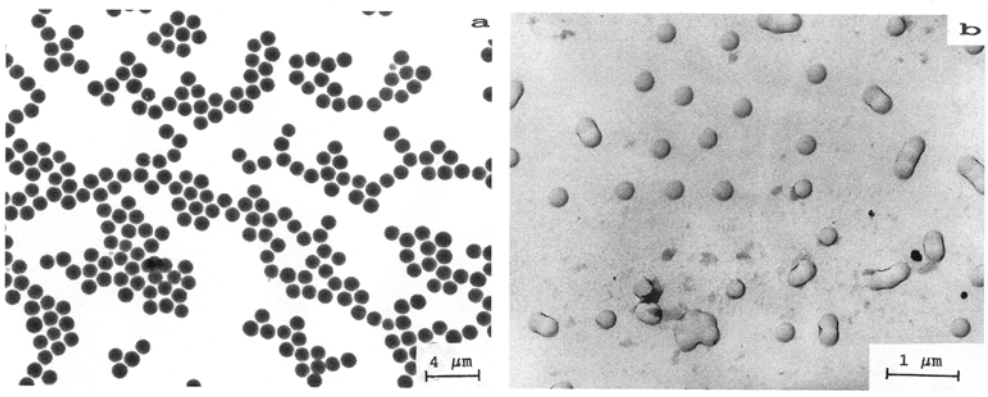

Fig. 3 Electron micrographs of a) PS particles (direct TEM), radius 601 nm b) PBMA particles (replica), radius 167 nm

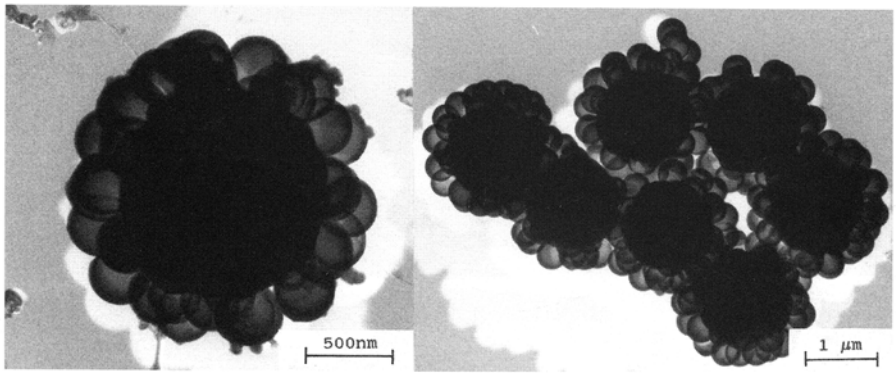

Fig. 4 Electron micrographs of freeze-dried heterocoagulated samples showing small cationic PBMA particles adsorbed onto large PS particles for the condition N_{sat}

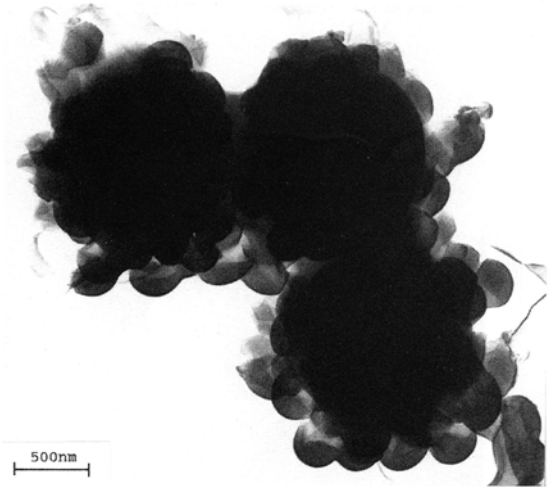

Fig. 5 Electron micrographs of heterocoagula prepared under conditions corresponding to N_{sat} after heating to 70 °C (freeze-dried replicas)

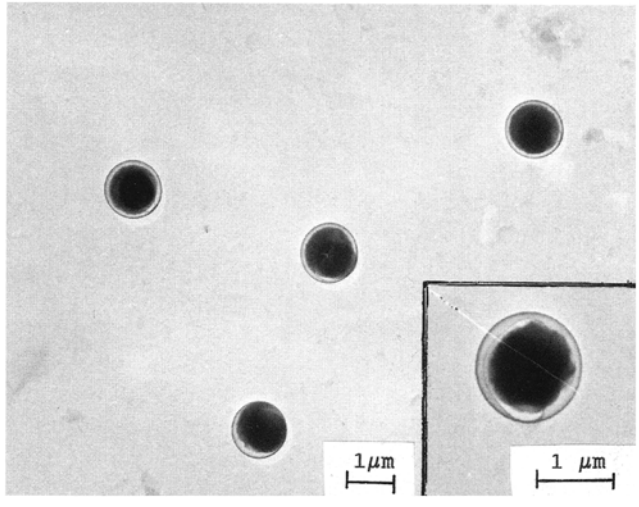

Fig. 6 Replica transmission electron micrographs of particles after heterocoagulation, using conditions corresponding to N^* at 25 °C, and then heating to 70 °C. Dark inner region, core PS: Light outer region, shell PBMA

Electrophoresis

The basic PS and PBMA latices and the composite latex prepared under N^* conditions were all examined by electrophoresis over the pH range of ca 2 to 10. The results obtained are illustrated in Fig. 7. The examination of the initial latices was carried out in order to determine the pH condition which was appropriate to mix the PS and

© Steinkopff Verlag 1997

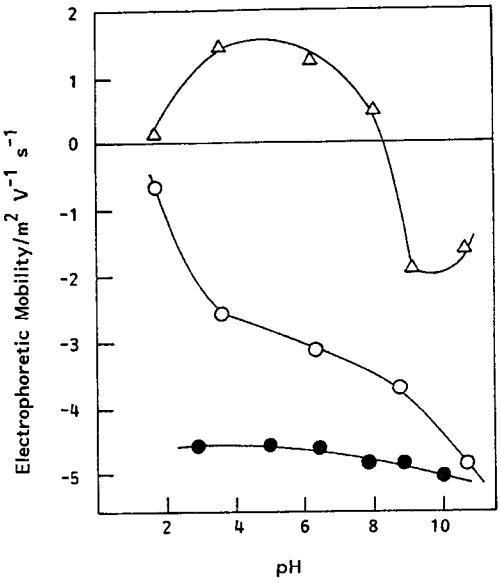

Fig. 7 Electrophoretic mobility against pH for, —○—, PS core particles; —△—, PBMA encapsulating particles; —●—, composite core-shell particles. Basic electrolyte content at ca pH 7, 10^{-3} mol dm^{-3} sodium chloride

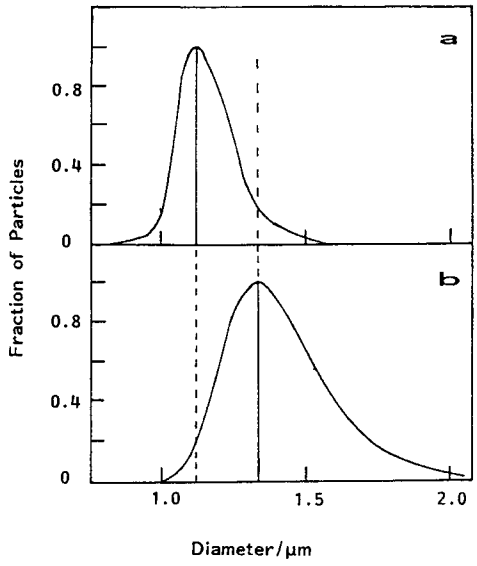

Fig. 8 Traces obtained using disc centrifuge photosedimentometry for a) PS core particles b) composite core (PS) + shell (PBMA) particles

PBMA latices. The cationic latices were found to have an isoelectric point at pH 8.3 ± 0.1, similar to that found in previous work [4, 6], and hence the PBMA particles were positively charged below this; the PS particles were negatively charged over the pH range examined. In order to carry out the heterocoagulation experiments the pH was adjusted to pH 5.0 ± 0.3.

The composite latex, which was examined in 10^{-5} mol dm^{-3} sodium chloride solution exhibited a negative electrophoretic mobility over the pH range examined as shown in Fig. 7. This result was somewhat surprising. However, it is clear from the electron micrograph shown in Fig. 6 that during the conversion from the N^* heterocoagulated condition to the composite core-shell particle a considerable change has occurred with the PBMA in that it is now a thin layer of polymer and not in a particulate form. Moreover, it seems reasonable to suppose that neutralisation of the negative charges on the PS by the residual positive charges on the PBMA would play a rôle in the spreading process and help to produce adhesion at the interface between the two polymers. Also, some experimental evidence, such as the freeze-thaw stability of the composite particles indicated that the surface of the composite particles was coated with MeOPEGMA thus enabling the hydrophilic character of the surface to be maintained.

Disc centrifuge photosedimentometry

Figure 8 shows the traces obtained by disc centrifuge photo-sedimentometry for the PS core particles and for composite particles obtained under N^*. These traces were obtained using the previously measured value of 1.055 ± 0.001 g cm^{-3} for the density of PS [44], which was in close agreement with literature values [46], and a value of 1.038 ± 0.001 g cm^{-3} for the composite particles, which was measured using an Anton Paar density meter.

The shift in the mode of the curve following encapsulation to a weight average diameter of 1.33 μm from that of the original PS latex of 1.15 μm is clearly visible. Moreover, the change in polydispersity as measured by the weight average/number average index to 1.045 from 1.019 indicated that the composite particles were still reasonably monodisperse.

Discussion

The experiments reported in the present work have shown that, starting with a latex of anionic PS particles and a latex of cationic PBMA particles with grafted chains of MeOPEG also on the surface, these can be mixed at a pH of 5.0 ± 0.3 in order to heterocoagulate the PBMA particles on to the large PS particles. On heating these particles 45 °C above the glass-transition temperature of the PBMA particles the latter spread to encapsulate the PS core particle with a shell of PBMA. The final encapsulated

particles appeared to be sterically stabilised. This provides a novel approach to the preparation of well-defined core-shell particles which seems to have potential applications well beyond the scope of the present limited investigation.

Electrophoresis experiments shows that the cationic particles whose charge originated from the amidine end-groups on the surface, had an isoelectric point at pH 8.3 ± 0.1 (Fig. 7). However, evidence both in this work and in previous work [4, 6] has indicated that the amidine groups appear to be subject to hydrolysis under alkaline conditions according to the mechanism suggested below.

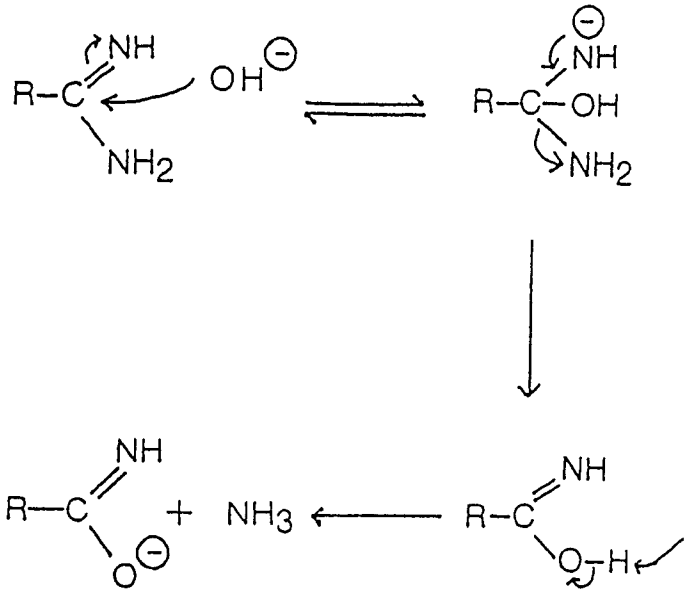

Hence, partly for this reason MeOPEG chains were used to ensure colloid stability of the latices.

The electrostatic colloidal stability of the systems used can be considered in the following way using the basic theory of Derjaguin and Landau [47] and Verwey and Overbeek [48] as extended by Hogg, Healy and Fuerstenau [49] for particles of radii R_1 and R_2 and surface potentials ψ_1 and ψ_2. This gives the electrostatic interaction energy for hetero-interaction as,

$$V_R = \frac{\pi\varepsilon_r\varepsilon_0 R_1 R_2}{4(R_1+R_2)}(\psi_1^2+\psi_2^2)\left[\left(\frac{2\psi_1\psi_2}{\psi_1^2+\psi_2^2}\right)\times\ln\left(\frac{1+\exp(-\kappa h)}{1-\exp(-\kappa h)}\right)+\ln(1-\exp(-2\kappa h))\right] \quad (4)$$

with ε_r the relative permittivity of the medium, ε_0 the permittivity of free space and κ the reciprocal double-layer thickness of the bulk electrolyte which for a 1:1 electrolyte is given by

$$\kappa^2 = 2cN_{AV}e^2v^2/\varepsilon_r\varepsilon_0 kT$$

with e the charge on the electron, N_{AV} Avogadro's number, c the electrolyte concentration in mol m^{-3} and v the magnitude of the ion charges. h = the surface–surface separation distance.

For homoelectrostatic interaction $R_1 = R_2$ and $\psi_1 = \psi_2$. In the present work the electrophoretic mobilities were measured and converted into zeta-potentials [50] and assuming these equivalent, for present purposes, to the surface potentials we obtain from the electrophoretic mobility data Fig. 7, $\psi_1 = +18$ mV ($R_1 = 167$ nm) and $\psi_2 = -38$ mV ($R_2 = 601$ nm).

The van der Waals' attractive energy between two spheres of different sizes was given by Hamaker [51] as

$$V_A = -\frac{A_c}{12}\left[\frac{y}{x^2+xy+x}+\frac{y}{x^2+xy+x+y}+2\ln\frac{x^2+xy+x}{x^2+xy+x+y}\right] \quad (5)$$

where $x = h/2R_1$ and $y = R_2/R_1$. A_c is the composite Hamaker Constant for the particles in the medium. This was taken as the value for polystyrene, 0.95×10^{-20} J [51].

The curves in Fig. 9 were calculated using the figures quoted above. Firstly, the curves for homointeractions are shown in Fig. 9a. It is clear that the anionic particles have a strong electrostatic repulsion and are therefore quite stable. The electrostatic interaction between the cationic particles based on $\psi_1 = 18$ mV is rather weak and suggests that the charge, in itself, was not adequate to produce significant colloid stability. However, these particles were prepared with a surface layer of methoxy polyethylene glycol as a steric stabiliser. Consequently, assuming this material to have an extended conformation of 10 nm, based on a molecular mass of 2000 and, for present purposes, taking the steric interaction as that of hard-spheres we can place a vertical interaction line [58] for the steric term, V_S at 20 nm. In view of the low surface potential of the cationic particles it is clear that the steric term makes a major contribution to their colloid stability.

The curve for heterointeraction ($V_R + V_A$) between the anionic and cationic particles is shown in Fig. 9b based on data for two particles of radii 167 and 601 nm and surface potentials of +18 mV and −38 mV. As anticipated the heterointeraction is strongly attractive and leads to heterocoagulation as indicated in Figs. 4 and 5; The Vold effect [54], which is small for this situation, has not been included in the calculations of the attraction. However, since the cationic particles have a steric barrier as well as a weak cationic charge this needs to be taken into account. Again assuming as a primitive model, a hard interaction

© Steinkopff Verlag 1997

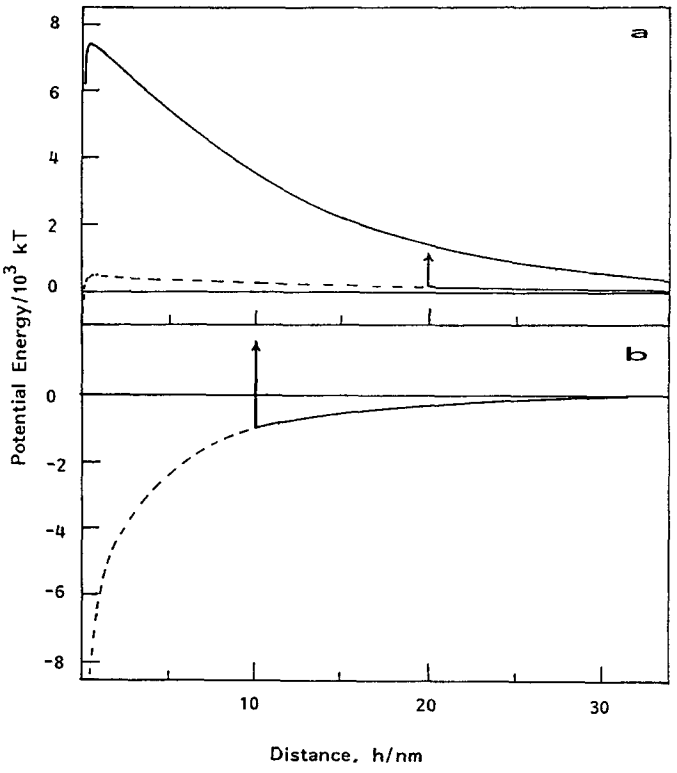

Fig. 9 Potential energy against distances of surface separation between original interacting particles: a) ——, $V_R + V_A$ for PS particles; – – –, $V_R + V_A$ for PBMA particles; ↑, onset of "hard-sphere" steric interaction term V_S. b) – – –, $V_R + V_A$ for heterointeraction between PS and PBMA particles; ↑, onset of "hard-sphere" steric interaction

and an extended length of 10 nm, this can be represented by a vertical line at 10 nm; i.e., V_S, taking the total interaction energy as,

$$V_T = V_R + V_A + V_S .$$

This effect substantially reduces the depth of the energy well in the close approach of the cationic and anionic particles. Thus the layer of MeOPEG molecules grafted onto the PBMA surface also seems to play an important part in the overall process. Firstly, at the lower temperature of 25 °C, as mentioned, when the particles are synthesized it provides steric stabilisation to the cationic particles as well as charge stabilisation. Then during the heterocoagulation process although it is the attraction between opposite charges which brings the particles together the steric barrier prevents close contact between the coating particle and the core particle thus allowing some surface mobility for the PBMA particles. This lateral mobility probably also helps the PBMA particles to form a more uniform coating on the core particle surface.

In addition, on heating to 70 °C the MeOPEG chains undergo some desolvation and hence become more hydrophobic (or oleophilic). As a consequence the steric layer is likely to contract and allow the PBMA particles to approach the core particles more closely. The coating PBMA particles can also approach each other more closely and with the increased chain flexibility and motion at 70 °C, spreading on the core particle can occur (Eq. (1)) followed by coalescence to form a shell of PBMA on the core.

On returning to 25 °C any MeOPEG groups remaining on the shell surface can resolvate and thus contribute to the colloid stability of the composite particles.

Although heterocoagulation was found, as previously [7, 8] and as predicted above to be a facile process, an important discovery in the present work is that the number of particles packed on the surface appears to play a major rôle when heterocoagulation is used as a precursor to encapsulation. With a close-packed layer on the surface, N_{sat}, as defined in the theory section, the coalescence process at 70 °C was unsatisfactory. However, when the packing conformed to N^*, so that the total area of the coating particles equalled that of the final encapsulated particle, then a uniform shell was observed after raising the heterocoagulated units 45 °C above the glass-transition temperature of the PBMA particles.

A surprising effect observed in the present work was that the electrophoretic mobility of the final composite particles was negative and indicated a zeta-potential of ca. – 55 mV on the particles. Possible effects which could occur to explain this result include complete hydrolysis of the amidine group at 70 °C and/or some migration of low molecular weight species with anionic end-groups from the PS particles to the surface of the composite particles. This effect needs further investigation.

Acknowledgments We wish to express our thanks to ICI Paints for support of this work from the Strategic Research Fund. We also wish to thank Mrs. Anne Robinson and Mr. Roy Buckley for help with the cryoscopic electron microscopy, and Dr. S. Downing for a number of useful discussions. One of us (RHO) also acknowledges with thanks support from the DTI Colloid Technology programme.

References

1. Upton RW (1952) US Patent 2599300
2. Hammond GS, Neumann RG (1963) J Amer Chem Soc 85:1501
3. Breitenbach JW, Kuchner K (1966) Monashefte Chem 97:662
4. Pelton R (1976) Thesis University of Bristol

5. Goodwin JW, Ottewill RH, Pelton R, Vianello G, Yates DE (1978) Brit Polymer J 10:173
6. Goodwin JW, Ottewill RH, Pelton R (1979) Colloid Polym Sci 257·61
7. Goodwin JW, Ottewill RH (1978) Faraday Disc Chem Soc 65:338
8. Cheung WK (1979) Thesis University of Bristol
9. Ottewill RH (1982) In Piirma, Emulsion Polymerisation. Academic Press, pp 36–38
10. Waters JA (1990) US Patent 5210113
11. Waters JA (1993) European Patent 0327199
12. Waters JA (1993) European Patent 5296524
13. Okubo M, Ichikawa K, Tsujihiro M, He Y (1990) Colloid Polym Sci 268:791
14. Okubo M, He Y, Ichikawa K (1991) Colloid Polym Sci 269:125
15 Okubo M, Miyachi N, Lu Y (1994) Colloid Polym Sci 272:270
16. Ottewill RH, Schofield AB, Waters JA (1996) Colloid Polym Sci 274:763
17. Daniel JC (1985) Makromol Chem Suppl 10/11:359
18. Vanderhoff JW, Dimonie V, El-Aasser MS, Klein E (1985) Makromol Chem Suppl 10/11:391
19 Sutterlin N (1985) Makromol Chem Suppl 10/11:403
20. Lee DI, Ishikawa T (1983) J Pol Sci Pol Chem Ed 21:143
21 Cho I, Lee DI (1985) J Appl Pol Sci 30:1903
22. Okubo M, Ando M, Yamada A, Katsuta Y, Matsumoto TJ (1981) J Pol Sci Lett Ed 19:143
23. Bootle GA, Lye JE, Ottewill RH (1990) Makromol Chem Makromol Symp 35/36·291
24. Okubo M, Yamada A, Matsumoto A (1990) J Pol Sci Pol Chem Ed 22:3219
25. Jonsson JEL, Hassander H, Jansson LH, Tornell B (1991) Macromolecules 24:126
26. Lee S, Rudin A (1992) ACS Symposium Series 492·234
27. Vandezande GA, Rudin A (1992) ACS Symposium Series 492:119
28. Chen YC, Dimonie V, El-Aasser MS (1992) J Appl Polymer Sci 45:487
29. Vandezande GA, Rudin A (1992) ACS Symposium Series 492:119
30. Fitch RM (1995) Makromol Symp 92:1
31. Rudin A (1995) Makromol Symp 92:53
32. Berg J, Sundberg DC, Kronberg B (1986) Polym Mater Sci Eng 54:367
33. Berg J, Sundberg D, Kronberg B (1989) J Microencapsulation 6:327
34. Sundberg DC, Casassa AP, Pantazopoulos J, Muscato MR (1990) J Appl Polymer Sci 40:1425
35. Sundberg DC, Durant YG (1995) Makromol Symp 92:43
36. Waters JA (1994) Colloids and Surfaces 83:167
37. Waters JA (1995) In: Goodwin JW, Buscall R (eds) Colloidal Polymer Particles. Academic Press, London, p 113
38. Roulstone BJ, Waters JA (1994) European Patent 549:163
39. Ottewill RH, Satgurunathan R, Westby MJ (1987) Br Polym J 19:435
40. Ottewill RH, Satgurunathan R (1987) Coll Polym Sci 265:845
41. Goodwin J, Hearn J, Ho CC, Ottewill RH (1974) Coll Polym Sci 252:464
42. Johnson K (1995) PhD thesis, University of Bristol
43 Bandrup EH (1975) In: Immergut (ed) Polymer Handbook. Wiley – Interscience, New York
44. Lye JE (1988) PhD thesis, University of Bristol
45. Ottewill RH, Rennie AR, Schofield AB, Waters JA (1996) to be published
46. Bateman JB, Weneck EJ, Eshler OC (1969) J Coll Int Sci 14:308
47 Derjaguin BV, Landau L (1941) Acta Physichim URSS 14:633
48. Verwey EJW, Overbeek, JThG (1948) Theory of Stability of Lyophobic Colloids, Elsevier, Amsterdam
49. Hogg R, Healy TW, Fuerstenau DW (1966) Trans Faraday Soc 62:1638
50. O'Brien RW, White LR (1978) J Chem Soc Faraday II 74:1607
51. Hamaker HC (1937) Physica 4:1058
52. Hough DB, White LR (1980) Advances Colloid Int Sci 14:3
53. Goodwin JW, Ottewill RH (1991) J Chem Soc Faraday Trans 87:357
54. Vold MJ (1961) J Coll Sci 16:1